environmental microbiology

Environmental Microbiology (2015) **17**(8), 2735–2746 doi:10.1111/1462-2920.12711

A small molecule species specifically inhibits *Fusarium* myosin I

Chengqi Zhang,[1†] Yun Chen,[1†] Yanni Yin,[1] Huan-Hong Ji,[2] Won-Bo Shim,[3] Yiping Hou,[4] Mingguo Zhou,[4*] Xiang-dong Li[2*] and Zhonghua Ma[1*]

[1]*Institute of Biotechnology, Zhejiang University, Hangzhou 310058, China.*

[2]*National Laboratory of Integrated Management of Insect Pests and Rodents, Institute of Zoology, Chinese Academy of Sciences, Beijing 100101, China.*

[3]*Department of Plant Pathology and Microbiology, Texas A&M University, College Station, TX 77843-2132, USA.*

[4]*Department of Plant Pathology, Nanjing Agricultural University, Nanjing 210095, China.*

Summary

***Fusarium* head blight (FHB) caused by *Fusarium graminearum* is a devastating disease of cereal crops worldwide. Recently, a novel fungicide JS399-19 has been launched into the marketplace to manage FHB. It is compelling that JS399-19 shows highly inhibitory activity towards some *Fusarium* species, but not to other fungi, indicating that it is an environmentally compatible fungicide. To explore the mode of action of this species-specific compound, we conducted a whole-genome transcript profiling together with genetic and biochemical assays, and discovered that JS399-19 targets the myosin I of *F. graminearum* (FgMyo1). FgMyo1 is essential for *F. graminearum* growth. A point mutation S217L or E420K in FgMyo1 is responsible for *F. graminearum* resistance to JS399-19. In addition, transformation of *F. graminearum* with the myosin I gene of *Magnaporthe grisea*, the causal agent of rice blast, also led to JS399-19 resistance. JS399-19 strongly inhibits the ATPase activity of the wild-type FgMyo1, but not the mutated FgMyo1$^{S217L/E420K}$. These results provide us a new insight into the design of species-specific antifungal compounds. Furthermore, our strategy can be applied to identify novel drug targets in various pathogenic organisms.**

Introduction

Fusarium head blight (FHB) is a devastating disease of cereal crops worldwide caused by pathogenic *Fusarium* species, including *Fusarium graminearum* and *F. asiaticum* (Xu and Nicholson, 2009; Dean *et al*., 2012). In addition to severe yield losses, FHB leads to mycotoxin contamination in infested grains, e.g. deoxynivalenol (DON) and zearalenone, that poses a serious threat to human and animal health (Pestka and Smolinski, 2005; McMullen *et al*., 2012). In most cereal species, the resistance sources identified are major quantitative trait loci (QTL) based but unfortunately these are only partially effective (Steiner *et al*., 2009). Thus, the application of systemic fungicides, such as sterol demethylation inhibitors (DMIs) and the benzimidazoles (MBCs), has been one of the primary tools for controlling FHB (McMullen *et al*., 2012). It is not surprising that DMI- and MBC-resistant *Fusarium* species have been identified in several countries since these fungicides have been used extensively over the past two decades (Yin *et al*., 2009; Becher *et al*., 2010; Liu *et al*., 2010). The use of recently developed quinone outside inhibitors (QoIs) is frequently associated with greater DON concentrations in grain compared with non-treated wheat (Ramirez *et al*., 2004; Müllenborn *et al*., 2008), thus restricting the application of QoI fungicides for FHB management. Obviously, the lack of alternative chemicals and the emergence of DMI- and MBC-resistant *Fusarium* populations further underscore the need for the development of novel compounds against FHB.

Recently, a novel cyanoacrylate fungicide JS399-19 (2-cyano-3-amino-3-phenylancryic acetate) (Fig. S1A) was developed by the Jiangsu Branch of National Pesticide Research and Development Center of China and has been marketed for FHB management. This compound aggressively inhibits mycelial growth of *F. graminearum*, *F. moniliforme* and *F. oxysporum*, and it exhibits an excellent efficacy in controlling FHB in field trials (Li *et al*., 2008; Chen and Zhou, 2009; Zhang *et al*., 2010). Genetic analyses showed a major gene controlling the resistance to JS399-19 (Chen *et al*., 2009). Meanwhile, these

Received 5 September, 2014; revised 3 November, 2014; accepted 5 November, 2014. *For correspondence. E-mail zhma@zju.edu.cn; lixd@ioz.ac.cn or mgzhou@njau.edu.cn; Tel. (+86) 571 88982268; Fax (+86) 571 88982268. †These authors contributed equally to this work.

© 2014 Society for Applied Microbiology and John Wiley & Sons Ltd

JS399-19-resistant (JS-R) mutants remained sensitive to other commercial fungicides including DMIs and MBCs (Li *et al*., 2008). Moreover, JS399-19 was not effective against other ascomycete fungi including *Aspergillus flavus* and *Botrytis cinerea* (Li *et al*., 2008). These reports led us to hypothesize that JS399-19 has a species-specific mode of action against Fusaria, and our aim here was to investigate and define this novel mechanism.

Elucidating the precise biological mode of action for a chemical compound is often highly challenging. Traditional affinity 'pull down' strategies have been successful in identifying the protein targets of a number of compounds (Sato *et al*., 2010). However, these approaches have critical drawbacks: (i) numerous compounds cannot readily be grafted onto a solid matrix, or cannot maintain their affinity for protein targets once immobilized, and (ii) compounds that irreversibly or covalently modify their targets do not release targets during column wash (Azad and Wright, 2012). Recently, whole-genome transcript profiling has emerged as a valuable tool to investigate effects of bioactive compounds on various microorganisms. By comparing the list of altered transcripts, we can predict altered genetic pathways in an organism due to the application of a chemical compound. However, it is difficult to identify genetic targets that are direct targets of the compound with a simple analysis of gene transcript profiles (Palchaudhuri and Hergenrother, 2011). To overcome this drawback, we conducted comprehensive analyses of gene expression profiles for JS399-19-sensitive (JS-S) and JS-R strains of *F. graminearum* subjected to JS399-19 treatment. It is reasonable to expect that the application of antifungal compound induce differential expression of genes in sensitive and resistant strains resulting in altered physiological responses. With this premise, we found 156 genes significantly upregulated in a JS-S strain but not in JS-R mutant treated with JS399-19. After comparing the sequences of these 156 genes in JS-S and JS-R strains, we discovered that all JS-R mutants tested contain a point mutation at the codon 217 or 420 in myosin I (gene locus FGSG_01410). Genetic and biochemical analyses showed that JS399-19 targets myosin I and inhibits the ATPase activity of *F. graminearum* myosin I. Results of this study indicate for the first time that myosin I is a novel drug target and thus provide new strategies for the development of species-specific compound against pathogenic Fusaria.

Results

JS399-19 is highly active against some but not all Fusarium *species*

To explore the target of JS399-19, we first compared the activity of JS399-19 against two *Fusarium* species with other two commercial carbendazim and tebuconazole fungicides, which have been applied widely for FHB management. Sensitivity test showed that JS399-19 exhibits stronger inhibitory activity against *F. graminearum* (PH-1 strain) and *F. asiaticum* (GJ33 strain) than carbendazim and tebuconazole (Fig. S1B). Furthermore, we have tested more than 10 000 isolates of *F. graminearum* and *F. asiaticum* collected from various locations in China for JS399-19 sensitivity in the last several years, and found that all of them were highly susceptible to this compound (Gao, Q. and Ma, Z., unpubl. data). In contrast, JS399-19 showed a low or even no activity against mycelial growth of other species including pathogenic fungi *Fusarium solani*, *Magnaporthe grisea*, *B. cinerea*, *A. flavus* and the budding yeast *Saccharomyces cerevisiae* (Fig. 1). In addition, microscopic examination revealed that JS399-19 also inhibited conidial germination and germ tube elongation in *F. graminearum*. However, JS399-19 at 50 $\mu g\ ml^{-1}$ showed little effects on conidial germination in *M. grisea* (Fig. S2). These results indicated that the antifungal activity of JS399-19 is specific to some *Fusarium* species.

Transcriptional profiling analysis of potential target gene of JS399-19

Fusarium graminearum was unable to grow on potato dextrose agar (PDA) amended with 10 $\mu g\ ml^{-1}$ tebuconazole for 2 days, but showed a slight growth after 4 days of incubation (Fig. 2A). Carbendazim showed sustainable inhibition against *F. graminearum*; the fungus was not capable of growing on PDA amended with 10 $\mu g\ ml^{-1}$ carbendazim up to 7 days of incubation (Fig. 2B). Previous studies showed that tebuconazole can induce overexpression of *CYP51* genes (encoding C14α-methylases, which are the targets of tebuconazole) in *F. graminearum* (Becher *et al*., 2011; Liu *et al*., 2011). However, carbendazim treatment does not induce overexpression of its target gene (beta-tubulin gene) (Fig. S3). Similar to the culture treated with tebuconazole, *F. graminearum* showed a sign of growth after 4 days of incubation on PDA amended with 10 $\mu g\ ml^{-1}$ JS399-19 (Fig. 2A), suggesting that JS399-19 may induce overexpression of its target gene(s) in *F. graminearum*. Meanwhile, a previous study suggested that the resistance of *F. graminearum* to JS399-19 is due to a single major gene (Chen *et al*., 2009). Thus, our hypothesis was that the target gene is upregulated significantly in a JS-S strain but not in a JS-R mutant subjected to JS399-19 treatment. We first obtained 10 JS-R mutants by ultraviolet (UV) mutagenesis, selecting for strains that grew well on PDA amended with 100 $\mu g\ ml^{-1}$ JS399-19 after 2 days of incubation (Fig. S4A). In contrast, the wild-type (WT) strain PH-1 was unable to grow even at 1 $\mu g\ ml^{-1}$. Subsequently, we compiled genome-wide transcriptional

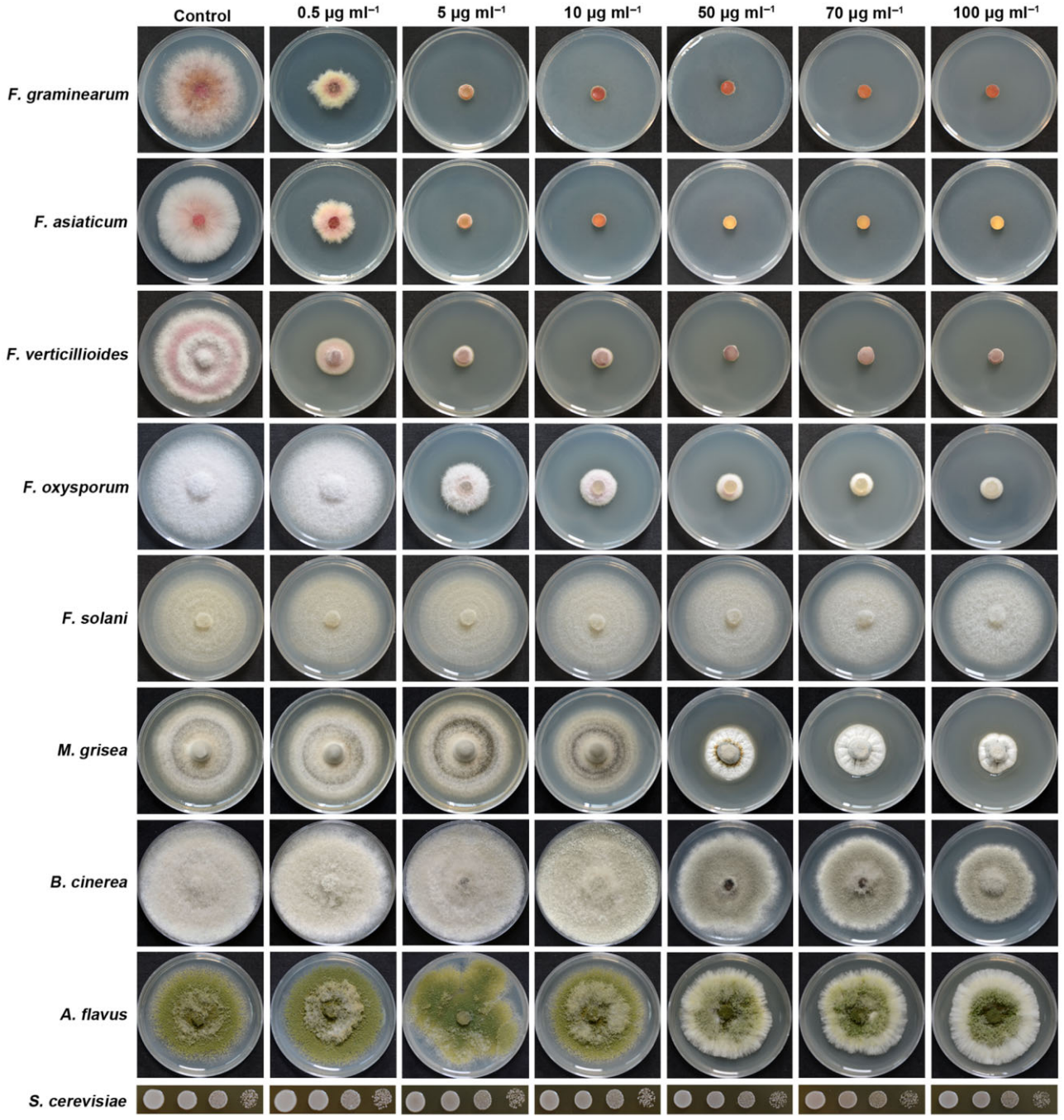

Fig. 1. Antifungal activity of JS399-19 against *Fusarium graminearum*, *Fusarium asiaticum*, *Fusarium verticillioides*, *Fusarium oxysporum*, *Fusarium solani*, *Magnaporthe grisea*, *Botrytis cinerea*, *Aspergillus flavus* and *Saccharomyces cerevisiae*. *F. graminearum*, *F. asiaticum*, *F. verticillioides*, *F. oxysporum*, *F. solani*, *M. grisea*, *B. cinerea* and *A. flavus* were inoculated on PDA plates supplemented with various concentrations of JS399-19 as indicated in the figure. The inoculated plates were incubated at 25°C and imaged when mycelia on the control plate extended to the edge of plate. *S. cerevisiae* was grown on the YPAD plate amended with JS399-19 and incubated at 30°C for 3 days before imaging. The solvent dimethylsulphoxide (DMSO) was used as a negative control.

profiles for the WT PH-1 and JS-R strain (JS-R1) treated with JS399-19 at 0.5 μg ml^{-1} (a concentration of the EC_{90} value against PH-1) for 6 h (Fig. 2B). By comparing the gene expression profiles, we identified 156 genes that were upregulated more than eightfold in PH-1 compared with those in JS-R1 (Table S1). We sequenced these 156 genes from both PH-1 and JS-R1, and found that JS-R1 contained a point mutation from 'TCA' (serine) to 'TTA'

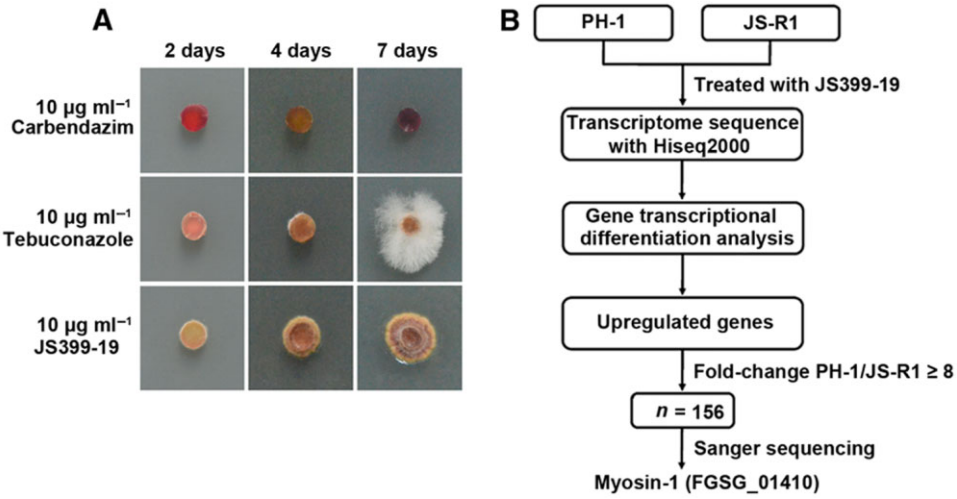

Fig. 2. Identification of the potential target gene of JS399-19.
A. Mycelial growth of *F. graminearum* PH-1 on PDA plates supplemented with carbendazim, tebuconazole and JS399-19 at final concentration of 10 μg ml^{-1}. Photos were taken 2, 4 and 7 days after inoculation at 25°C.
B. Strategy to identify putative target gene of JS399-19 by transcription profiling assays.

(leucine) at codon 217 in myosin I gene (hereafter referred as *FgMYO1*). Sequence analyses showed that all remaining nine JS-R mutants contained a point mutation either at the codon 217 or 420 in FgMyo1 (Fig. S4B). FgMyo1 contains three domains, i.e. the motor domain, two isoleucine and glutamine (IQ) motif, and C-terminal tail containing an SH3 motif (Fig. S4C). Based on the crystal structure of *Dictyostelium discoideum* myosin IE motor domain (Protein Data Bank (PDB) code: 1LKX), the two mutated residues S217L and E420K are adjacent to each other in the 50 kDa cleft of the motor domain in FgMyo1 (Fig. S4D). Based on the fact that a point mutation in the target gene is the most common fungicide resistance mechanism in pathogenic fungi (Ma and Michailides, 2005), we hypothesized that FgMyo1 is the target of JS399-19.

A point mutation in FgMyo1 *confers* F. graminearum *resistance to JS399-19*

To further verify whether the resistance of *F. graminearum* to JS399-19 is caused by a point mutation (S217L or E420K) in FgMyo1, the mutated *FgMYO1* containing either S217L or E420K was introduced into the WT PH-1 strain. The resulting strains (designated PH-1 + FgMYO1^{S217L} and PH-1 + FgMYO1^{E420K}) were confirmed by Southern analyses (Fig. S5). In addition, the strain transformed with the WT *FgMYO1* (named PH-1 + FgMYO1^{WT}) without any point mutation was used as a control. As shown in Fig. 3, similar to the JS-R mutants (JS-R1 and JS-R2), PH-1 + FgMYO1^{S217L} and PH-1 + FgMYO1^{E420K} strains became resistant to JS399-19 and were able to grow on PDA amended with JS399-19 at the final concentration of 50 and 100 μg ml^{-1}. We obtained 95 and 71 transformants containing FgMyo1 with S217L and E420K, respectively, and all 166 transformants were resistant to JS399-19. However, all 86 transformants with the WT *FgMYO1* remained sensitive to JS399-19. These results strongly indicated that the point mutations S217L or E420K in FgMyo1 were responsible for the resistance of *F. graminearum* to JS399-19.

To examine the effect of JS399-19 on subcellular localization of FgMyo1, the WT and mutated *FgMYO1* fused with green fluorescent protein (GFP) were independently introduced into the WT strain PH-1. Microscopic examination showed that strong fluorescent signals of the WT FgMyo1^{WT}-GFP were observed at the tip of germinating tubes, while the GFP signals diminished dramatically after the treatment with 0.5 μg ml^{-1} JS399-19 for 3 h (Fig. 4). In contrast, the fluorescent signals of mutated proteins FgMyo1^{S217L}-GFP and FgMyo1^{E420K}-GFP at the tip of germinating tubes were not affected dramatically by JS399-19 treatment (Fig. 4). These results indicated that JS399-19 affects localization of the WT FgMyo1 but not the mutated protein.

Transformation of F. graminearum *with the myosin I gene from* M. grisea *(MgMYO1) led to JS399-19 resistance*

JS399-19 has a low level of activity against *M. grisea* and other several fungi (Fig. 1). Alignment analyses showed a number of divergences in amino acid sequences among myosin I orthologues from *F. graminearum*, *F. asiaticum*,

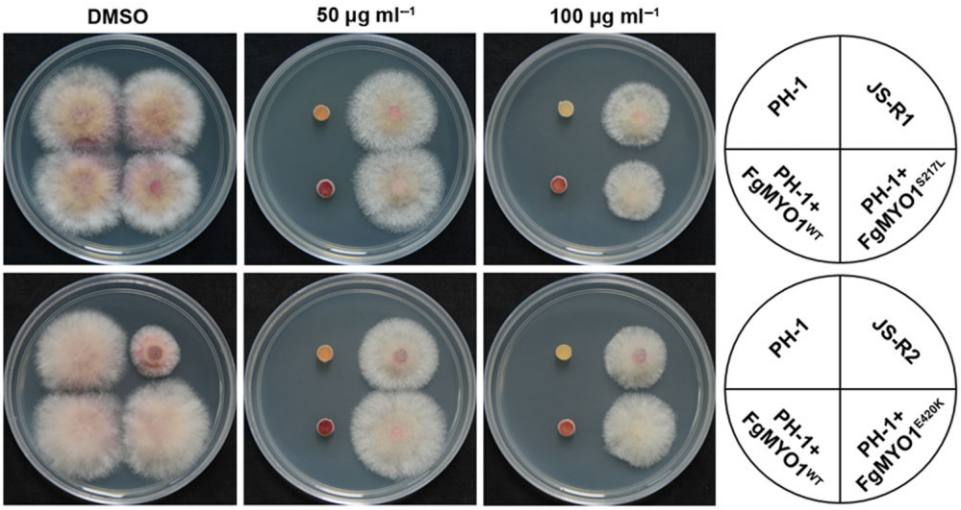

Fig. 3. The point mutations S217L and E420K in FgMyo1 are responsible for the resistance of *F. graminearum* to JS399-19. The JS399-19-resistant mutants JS-R1 and JS-R2, and the strains PH-1 + FgMYO1^{WT} (PH-1 transformed with the wild-type *FgMYO1*), PH-1 + FgMYO1^{S217L} (PH-1 transformed with the mutated *FgMYO1* containing the point mutation S217L) and PH-1 + FgMYO1^{E420K} (PH-1 transformed with the mutated *FgMYO1* containing the point mutation E420K) were inoculated on PDA plates without or with JS399-19 at the final concentration of 50 or 100 μg ml^{-1}. Dimethylsulphoxide (DMSO) (200 μl) was used as a control treatment.

F. solani and other fungi (Fig. S6). To explain why JS399-19 is not effective against other fungi, we transferred the WT *F. graminearum* strain PH-1 with *M. grisea* myosin I (*MgMYO1*) driven by the *FgMYO1* promoter. Three resulting transformants (named PH-1 + MgMYO1-1/-2/-3) were randomly selected from 72 transformants for phenotypic examinations. Sensitivity tests showed that all three transformants became resistant to JS399-19 (Fig. 5), indicating the divergences in MgMyo1 amino acids is responsible for *M. grisea* resistance to JS399-19.

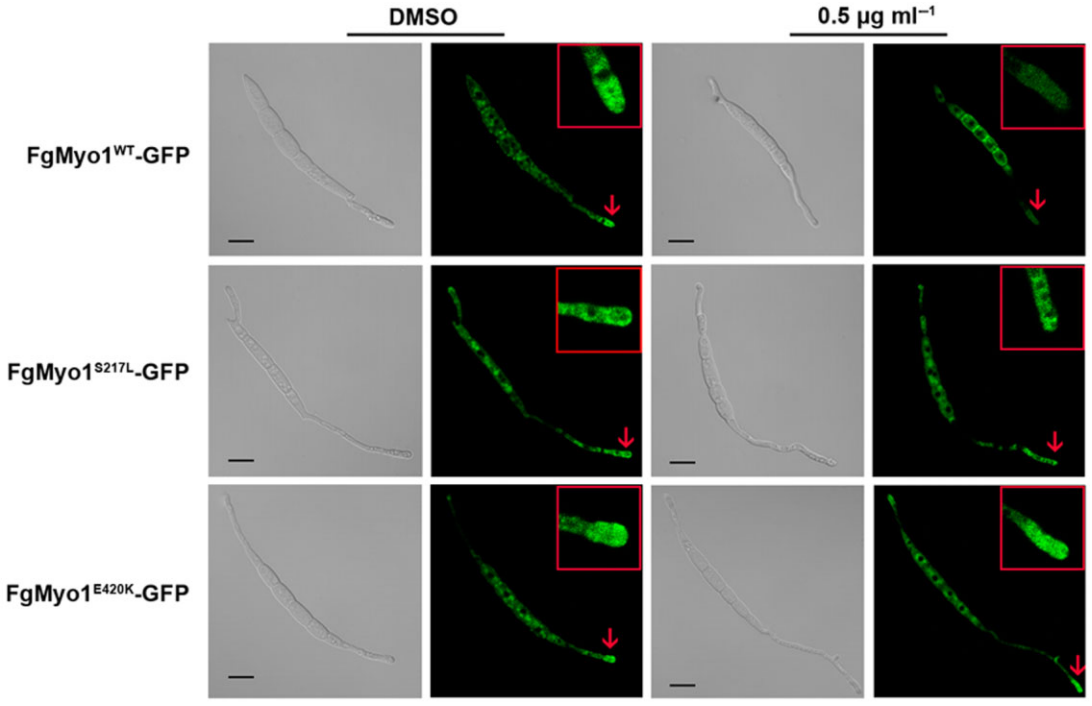

Fig. 4. Subcellular localization of FgMyo1 in germinating conidia. Conidia were incubated in 2% sucrose supplemented with 0.5 μg ml^{-1} JS399-19 at 25°C and imaged after 3 h treatment. The tips of germlings were enlarged for detailed observation. JS399-19 had a dramatically effect on localization of the wild-type FgMyo1 (FgMyo1^{WT}-GFP), but not on the mutated FgMyo1 (FgMyo1^{S217L}-GFP and FgMyo1^{E420K}-GFP) at the tips of germlings. Scale bars = 10 μm.

© 2014 Society for Applied Microbiology and John Wiley & Sons Ltd,

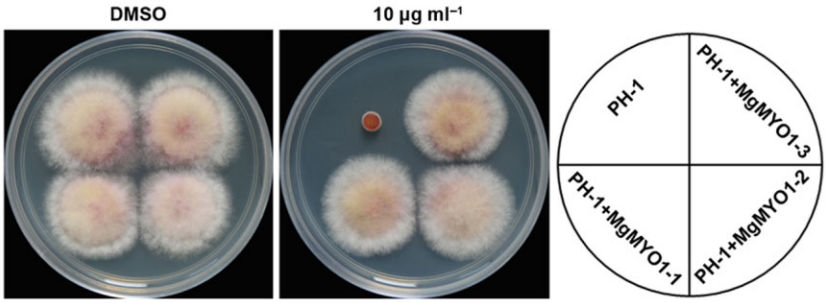

Fig. 5. *F. graminearum* strains bearing *Magnaporthe grisea* myosin I are resistant to JS399-19. Three *F. graminearum* transformants PH-1 + MgMYO1-1, PH-1 + MgMYO1-2 and PH-1 + MgMYO1-3 bearing *M. grisea* myosin I gene (*MgMYO1*) were inoculated on PDA plate supplemented with 10 μg ml^{-1} JS399-19. The same volume of dimethylsulphoxide (DMSO) (200 μl) was used as a control treatment. All inoculated plates were incubated at 25°C for 2 days before imaging. The wild-type PH-1 was used as a control strain.

FgMyo1 is essential for growth of F. graminearum

To investigate the biological function of FgMyo1 in *F. graminearum*, we targeted *FgMYO1* for gene deletion. We recovered 136 hygromycin-resistant transformants; however, all of them were ectopic mutants. The failure to obtain a *FgMYO1* null mutant despite the highly efficient homologous integration events in *F. graminearum* (Son *et al*., 2011; Wang *et al*., 2011) strongly indicated lethal effect of FgMYO1 deletion in this fungus. Myosin I has been described as essential in *Aspergillus nidulans* (McGoldrick *et al*., 1995).

To further explore the functions of FgMyo1, we were interested in phenotypic characterization of JS-R mutants. JS-R1, which contains the point mutation S217L, did not show detectable changes in hyphal growth, conidiation and virulence when compared with the WT PH-1 (Fig. 6A–C). In contrast, the mutant JS-R2, having the point mutation E420K, grew significantly slower than the WT on PDA. In addition, JS-R2 also exhibited significant defects in conidiation and virulence on wheat head (Fig. 6A–C). To confirm that phenotypic changes in JS-R2 were due to the point mutation E420K in FgMyo1, the mutated *FgMYO1*^{E420K} was introduced into the WT PH-1, and then the native WT *FgMYO1* was deleted from the transformant. Thus, the resulting mutant ΔFgMYO1+FgMYO1^{E420K} contained only the mutated *FgMYO1*^{E420K} in the WT PH-1. Consistent with the phenotype observed in JS-R2, ΔFgMYO1+FgMYO1^{E420K} showed various defects in hyphal growth, conidiation and virulence (Fig. 6A–C), indicating that the point mutation E420K impaired the biological functions of FgMyo1.

JS399-19 inhibits ATPase activity of FgMyo1 motor domain

To better understand how JS399-19 targets FgMyo1, we examined the effects of JS399-19 on the actin-activated ATPase activity of the FgMyo1 motor, which was overexpressed in sf9 cells and purified by affinity chromatography (Fig. S7). As shown in Fig. 7, the actin-activated ATPase activity of the WT FgMyo1 was inhibited by JS399-19 in a dose-dependent manner. Significantly, the activity was inhibited by more than 95% with 5 μg ml^{-1} JS399-19 treatment, indicating that JS399-19 is a potent inhibitor of FgMyo1 motor. In contrast, the actin-activated ATPase activity of FgMyo1-MIQ^{S217L} was only marginally inhibited by 5 μg ml^{-1} JS399-19 (~18%). As a negative control, the ATPase activity of FgMyo1 was not affected by the fungicide tebuconazole (5 μg ml^{-1}), which inhibits ergosterol biosynthesis (Liu *et al*., 2011). These results confirmed biochemically that JS399-19 targets FgMyo1, and the point mutation S217L in FgMyo1 is responsible for the resistance of *F. graminearum* to JS399-19. In addition, it is interesting that the actin-activated ATPase activity of FgMyo1-MIQ^{E420K} was very low (*circa* 5% as that of the WT FgMyo1) and was not inhibited by JS399-19 (Fig. 7). These results are in agreement with various defects observed in the JS-R mutant JS-R2.

Discussion

Class I myosins are widely expressed, single headed and membrane-associated members of the myosin superfamily that participate in regulating membrane dynamics and structure in nearly all eukaryotic cells (Liu *et al*., 2001; Laakso *et al*., 2008). In general, myosin I proteins function in a wide variety of cellular processes including polarized growth, cell motility, phagocytosis, endocytosis and exocytosis, and contractile vacuolar activity in various eukaryotic organisms (Kornt and Pollard, 1993; Durrbach *et al*., 1996; Temesvari *et al*., 1996; Mermall *et al*., 1998; Yamashita and May, 1998; Raposo *et al*., 1999; Lee *et al*., 2000; Neuhaus and Soldati, 2000; Oberholzer *et al*., 2002). The soil-living amoeba *D. discoideum* contains at least seven isoforms of class I myosins (MyoA-F and MyoK), but none of them are essential for growth. Studies of single gene deletion mutants of *D. discoideum* class I myosins indicate that there is a considerable overlap in function among them although they do not all perform exactly the same function (Osherov and May, 2000; Crawley *et al*., 2006). In *S. cerevisiae*, there are two highly related class I myosin genes, *MYO3* and *MYO5*. Deletion of either one results in no observable phenotypic

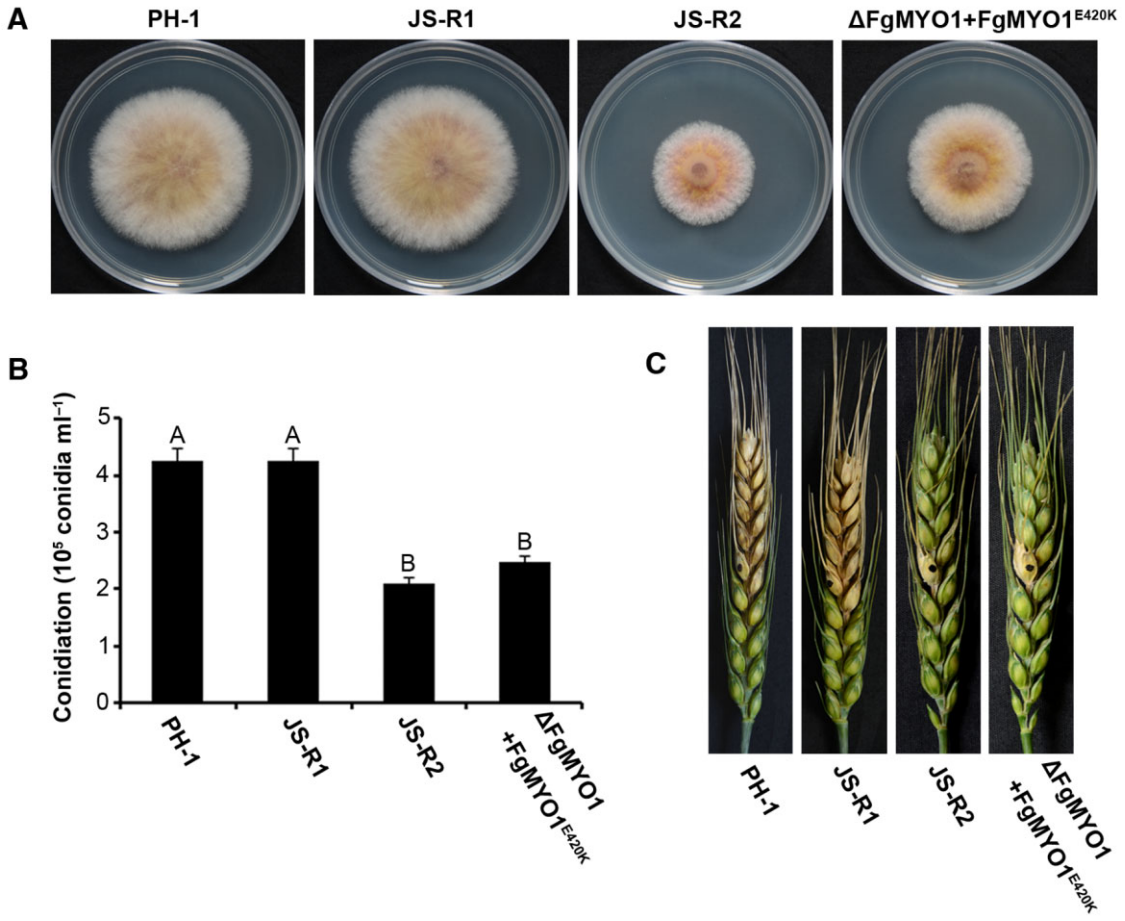

Fig. 6. Phenotypic analyses of *F. graminearum* strains containing the point mutation S217L or E420K in FgMyo1.
A. Colony morphology of the wild-type PH-1, the JS399-19-resistant mutants JS-R1 (containing the point mutation S217L), JS-R2 (having the point mutation E420K) and ΔFgMYO1+FgMYO1^{E420K} (the mutated *FgMYO1^{E420K}* was introduced into the wild-type PH-1, and the native wild-type *FgMYO1* was subsequently deleted from this strain) on PDA medium after 3 days incubation at 25°C.
B. Comparison of conidiation among PH-1, JS-R1, JS-R2 and ΔFgMYO1+FgMYO1^{E420K}. Each strain was incubated in CMC medium, and conidia were counted after 3 days of incubation at 25°C in a shaker. Values on the bars followed by the same letter are not significantly different at $P = 0.05$.
C. Disease symptoms on wheat head caused by the PH-1, JS-R1, JS-R2 and ΔFgMYO1+FgMYO1^{E420K}. Wheat heads were point inoculated with the conidial suspension of each strain, and infected wheat heads were examined 15 days after inoculation.

consequences, but deletion of both is either lethal (Geli and Riezman, 1996) or severely debilitating (Goodson *et al*., 1996). *Candida albicans* contains a single myosin I gene (*CaMYO5*). The *CaMYO5* mutant is viable but cannot form hypha (Oberholzer *et al*., 2002). The filamentous fungus *A. nidulans* also has a single myosin I, *MYOA*, but it is essential for *A. nidulans* growth (McGoldrick *et al*., 1995). Similar to *A. nidulans*, we learned that FgMyo1 is also essential for *F. graminearum* growth in this study. Therefore, specific inhibitors of myosin I proteins could act as a valuable tool in investigating many intracellular processes associated with myosin I in these fungi.

Although there have been considerable efforts to develop specific inhibitors of myosins, only few small-molecule myosin inhibitors with the functionality and specificity necessary for practical use have been identified to date (Bond *et al*., 2013). To our knowledge, an inhibitor of fungal myosin I has not been reported previously, and pentachloropseudilin (PCIP) is the only molecule that has been identified as an inhibitor of mammalian myosin I. This halogenated antibiotic reversibly inhibits both the ATPase activity and *in vitro* motility of myosin Ic and Ib of *Rattus norvegicus* with an IC_{50} value between 1 and 5 μM. In addition, PCIP selectively inhibits myosin-1c function in mammalian cells (Chinthalapudi *et al*., 2011). However, it is important to note that this compound also inhibits the ATPase activity of myosin Vb and non-muscle myosin II at higher concentrations (IC_{50} >90 μM). This lack of specificity at higher concentrations

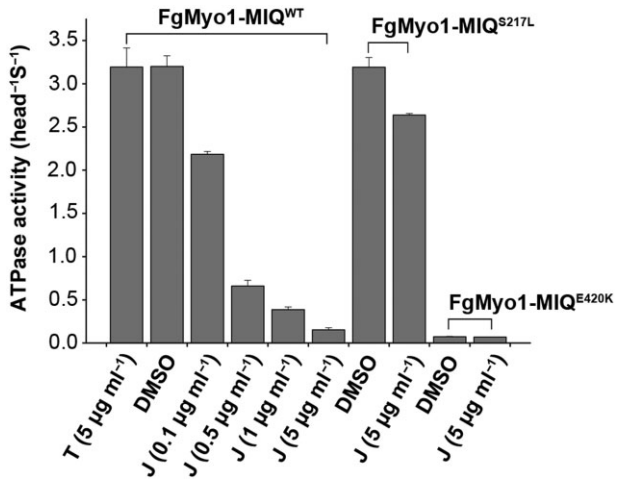

Fig. 7. The actin-activated ATPase activity of the wild type and mutated FgMyo1. ATP regeneration system was used to determine the inhibition of the actin-activated ATPase activity in FgMyo1-MIQ^{WT}, FgMyo1-MIQ^{S217L} and FgMyo1-MIQ^{E420K} induced by JS399-19 (abbreviated as 'J' in the figure label). Proteins were purified and adjusted to 0.1 μM. The solvent dimethylsulphoxide (DMSO) and tebuconazole (abbreviated as 'T' in the figure label) were used as control treatments. Bars denote standard errors from three repeated experiments.

must be taken into account when designing *in vivo* experiments using PCIP (Bond *et al*., 2013). In this study, we found that JS399-19 reveals highly inhibitory effect against the ATPase activity of Fg myosin I (Fig. 7). It is very interesting that this compound shows very low to no activity against mycelial growth of other fungi including *F. solani*, *M. grisea*, *A. flavus* and *S. cerevisiae*. Genetic transformation assay indicated that *F. graminearum* bearing *M. grisea* myosin I gene exhibited significantly increased resistance to JS399-19 (Fig. 5). Furthermore, JS399-19 has a very low level of oral toxicity against rat with LD_{50} greater than 5000 mg kg^{-1}, and this compound did not show any phytotoxicity (Wang *et al*., 2004). Taken together, these results indicated that JS399-19 is a specific inhibitor of some but not all *Fusarium* myosin I proteins.

Myosin I proteins contain head (motor), neck (IQ) and tail domains. The motor domain has an ATPase site and an ATP-sensitive F-actin-binding site. The neck domain binds one or more copies of a single light chain (often, but not always, calmodulin). The tail domain contains a basic subdomain, TH1, that binds to phospholipids and membranes (Liu *et al*., 2001). In this study, we found that JS-R mutants contain point mutations at the codon 217 and 420 in FgMyo1, which are located within the motor domain (Fig. S4D). ATPase activity assays showed that JS399-19 displayed very low levels of inhibitory activity against the myosin I with S217L and E420K point mutations. Interestingly, those two point mutations are located in the 50 kDa cleft of the motor domain. Therefore, we hypothesize that 50 kDa cleft is the binding site for JS399-19 and that the S217L or E420K mutation alters the conformation of 50 kDa cleft, thus preventing the binding of JS399-19. Further experiments are needed to determine the precise binding site of JS399-19 in *FgMyo1* and to clarify its inhibitory mechanism on *FgMyo1* function.

Experimental procedures

Strain constructions

Fusarium graminearum WT strain PH-1 (NRRL 31084) was used as the parental strain throughout this study. The *FgMYO1* deletion cassette was generated using the double-joint PCR strategy (Yu *et al*., 2004). The joined polymerase chain reaction (PCR) fragment or mutated *FgMYO1* was transformed into the WT PH-1 by polyethylene glycol (PEG)-mediated protoplast transformation method (Proctor *et al*., 1995). To construct the mutant ΔFgMYO1+FgMYO1^{E420K}, the 4.74 kb full-length DNA (including promoter region) of *FgMYO1^{E420K}* was cloned into the pYF11 plasmid using the Alkali-cation Yeast Transformation Kit (MP Biomedicals, Santa Ana, CA, USA) (Bruno *et al*., 2004). The recombination plasmid was transferred into the WT PH-1, and the resulting transformant (named PH-1 + FgMYO1^{E420K}) was confirmed by PCR assay. Subsequently, the native *FgMYO1* locus in PH-1 + FgMYO1^{E420K} was deleted by homologous recombination strategy to generate the mutant ΔFgMYO1+ FgMYO1^{E420K}. Single spore-isolated transformants growing on select drug-amended plates were verified by PCR (primers listed in Table S2) and Southern analyses (Fig. S5). The probe for Southern analyses were labelled with digoxigenin using the high prime DNA labelling and detection starter kit II according to the manufacturer's protocol (Roche Diagnostics, Mannheim, Germany).

Fungicides susceptibility evaluation

To test fungicide susceptibility, 5 mm (diameter) mycelial plugs of each strain were taken from the edge of a 3-day-old colony grown on PDA and were transferred onto PDA plates amended with JS399-19 or other fungicides at various concentrations as indicated in the figures. For each strain, three replicates per concentration were used. After the plates were incubated at 25°C for the time indicated in figure legends, the colony diameter in each plate was measured. Each experiment was repeated three times independently.

Induction of JS-R F. graminearum *mutants by UV irradiation*

In order to obtain JS-R mutants, 1×10^7 conidia of PH-1 were spread onto PDA plates supplemented with 100 μg ml^{-1} JS399-19, and then were exposed to UV (wavelength: 254 nm) light for 90 s which yielded a survival rate of 3.7×10^{-7}. After UV radiation, plates were incubated at 25°C for 4 days, and JS-R colonies growing on the plates were obtained. A total of 10 independent single-spore JS-R colonies were isolated for *FgMYO1* sequence analysis.

Transcription profiling assays for in the WT and JS-R mutant treated with JS399-19

To extract total RNA, mycelia of JS-R1 or PH-1 were inoculated into potato dextrose broth and cultured for 2 days at 25°C in the dark. Before mycelia were harvested for RNA extraction, each culture was treated with JS399-19 at final concentration of 0.5 μg ml^{-1} for 6 h. RNA from mycelia was extracted using a TaKaRa RNAiso Reagent (TaKaRa, Dalian, China) following the manufacturer's instruction. The RNA-seq libraries were constructed using the kit for digital gene expression-Tag profiling with DpnII (Illumina, San Diego, CA, USA) according to the manufacturer's protocol. The experiment was performed by BGI (Shenzhen, China) using Illumina Cluster Station and Illumina HiSeq 2000 System. Only tags with a frequency greater than 3 tag counts per million (tpm) were used in data analysis (Jongeneel *et al*., 2003). The unique tags were then aligned to all known transcripts of *F. graminearum* using Novoalign aligner (Novocraft Technologies, Kuala Lumpur, Malaysia). The frequencies of each sequenced tag in PH-1 and JS-R1 were compared.

Conidiation and virulence assays

For conidiation assay, fresh mycelia of each strain (50 mg) taken from the periphery of a 3-day-old colony were inoculated in a 50 ml flask containing 25 ml of carboxymethylcellulose (CMC) medium. The flasks were incubated at 25°C for 4 days in a shaker (180 r.p.m.). For each strain, the number of conidia in the broth was determined using a haemacytometer. Assays for virulence were performed as described previously (Jiang *et al*., 2011). Briefly, a 10 μl suspension of fresh conidia of each strain was injected into a floret in the central section spikelet of single flowering wheat head of susceptible cultivar Zimai22. There were 20 replicates for each strain. After inoculation, the plants were kept under 100% humidity at 22 ± 2°C for 2 days, and then maintained in a glasshouse. Fifteen days after inoculation, the infected spikelets in each inoculated wheat head were recorded. Each experiment was repeated three times.

Microscopic examinations of GFP fluorescence

To visualize the localization of FgMyo1 in *F. graminearum*, the *FgMYO1*^{WT} gene open reading fragment including the native promoter region was fused with carboxy-terminal GFP and transformed into PH-1 by PEG-mediated method as described previously (Jiang *et al*., 2011). In addition, FgMyo1^{S217L}-GFP and FgMyo1^{E420K}-GFP stains were also constructed. To observe FgMyo1 localization in germinating conidia, fresh conidia of each strain were incubated in 2% sucrose supplemented with 0.5 μg ml^{-1} JS399-19 and incubated at 25°C for 3 h. FgMyo1-GFP signals in germinating conidia were examined with the Zeiss LSM780 confocal microscope (Carl Zeiss AG, Jena, Germany).

Cloning, expression and purification of FgMyo1

To measure the inhibitory effect of JS399-19 towards actin-activated ATPase of FgMyo1, we expressed and purified the truncated FgMyo1 containing the motor and two IQ domains (residues 1–757, FgMyo1-MIQ) with Baculovirus/sf9 Expression System (Life Technology). The recombinant baculovirus expressing WT FgMyo1 (FgMyo1-MIQ^{WT}) was produced as follows. The cDNA fragment of FgMyo1-MIQ flanked by EcoRI and HindIII sites was amplified from PH-1 by PCR with the primers B13 + B14 (Table S2) and subcloned into pFast-HFTa (Lu *et al*., 2012). Recombinant baculovirus was prepared as described previously (Lu *et al*., 2012). Recombinant baculoviruses expressing FgMyo1-MIQ^{S217L} and FgMyo1-MIQ^{E420K} were prepared similarly, except that cDNA fragment was amplified from JS-R1 or JS-R2 respectively. All expressed FgMyo1-MIQ proteins have an N-terminal tag containing the sequence of hexa-histidine-tag and FLAG (a polypeptide protein tag DYKDDDDK)-tag to facilitate protein purification.

To express recombinant proteins, sf9 cells (1×10^9 per ml) were coinfected with recombinant viruses expressing FgMyo1-MIQ and calmodulin respectively, and the expressed proteins were purified as described previously (Li *et al*., 2004). Briefly, the infected cells were seeded in 15 flasks (175 cm^2) and cultured at 28°C for 3 days. Cells then were harvested and washed with 4 mM ethylene glycol tetraacetic acid (EGTA) in Tris Buffered Saline (TBS) (50 mM Tris-HCl, pH 7.5, 0.15 M NaCl). The resulting cell pellets were lysed with sonication in 30 ml of lysis buffer [50 mM Tris-HCl, pH 7.5, 0.3 M NaCl, 1 mM EGTA, 0.02% NaN_3, 5 mM ATP, 5 mM of 2-mercaptoethanol, 10 μg ml^{-1} leupeptin, 0.2 mg ml^{-1} trypsin inhibitor (egg) and 0.5% Triton X-100]. After centrifugation at 28 000 r.p.m. for 1 h, the supernatant was incubated with 1.0 ml anti-FLAG M2 affinity resin (Cat. A2220; Sigma, St Louis, MO, USA) in a 50 ml tube on a rotating wheel at 4°C for 2 h. The resin suspension was then loaded on a column (5 cm) and washed with 30 ml washing buffer (50 mM Tris-HCl, pH 7.5, 0.3 M NaCl, 0.2 mM EGTA, 2 μg ml^{-1} leupeptin and 5 mM of 2-mercaptoethanol). Target protein, bound to anti-FLAG agarose, was eluted with 0.1 mg ml^{-1} FLAG peptide in washing buffer and concentrated by Amicon® Ultratube (Millipore, Darmstadt, Germany). The collected proteins were dialysed overnight against 1 L buffer [5 mM Tris-HCl (pH 7.5), 0.2 M NaCl, 0.1 mM EGTA, 10% glycerol and 1 mM dithiothreitol (DTT)]. Protein concentration was determined by Coomassie brilliant blue R250 staining of SDS-PAGE (7.5–20%) using smooth muscle myosin heavy chain as a standard.

ATPase assay

We used an ATP regeneration system to measure the actin-activated ATPase activity of FgMyo1-MIQ^{WT}, FgMyo1-MIQ^{S217L} and FgMyo1-MIQ^{E420K}. The ATPase activity was measured at 25°C in a solution containing 0.1 μM myosin I, 20 mM MOPS (pH 7.0), 1 mM $MgCl_2$, 1 mM EGTA, 0.25 mg ml^{-1} BSA, 1 mM DTT, 2.5 mM phosphoenolpyruvate (PEP), 20 U ml^{-1} pyruvate kinase, 12 μM calmodulin, 150 mM NaCl, 0.5 mM ATP, 60 μM actin and various concentrations of JS399-19 as indicated in Fig. 7. The reaction was stopped at various times between 6 and 60 min by adding 100 μl reaction solution [0.3125 mM of 2, 4-dinitrophenyl hydrazine (Sigma) and 0.375 M HCl] to a 1.5 ml tube. After incubation at 37°C for 15 min, 50 μl stop solution (3.125 M

NaOH and 0.125 M EDTA) was added to each tube and absorption at 460 nm was recorded. The standard curve was measured using 0–0.5 mM freshly prepared pyruvate solution. The solvent DMSO and DMI fungicide tebuconazole (5 $\mu g\ ml^{-1}$) was used as the blank and negative controls respectively. The experiment was repeated three times. Analysis of variance was used to determine significant differences in ATPase activity among the treatments.

Acknowledgements

The research was supported by the National Key Basic Research and Development Program (2012CB114004), Special Fund for Agro-scientific Research in the Public Interest (No. 201303023) and China Agriculture Research System (CARS-3-1-15) to Z. Ma, and the National Key Basic Research and Development Program (2012CB114102) to X. Li.

References

Azad, M.A., and Wright, G.D. (2012) Determining the mode of action of bioactive compounds. *Bioorg Med Chem* **20:** 1929–1939.

Becher, R., Hettwer, U., Karlovsky, P., Deising, H.B., and Wirsel, S.G. (2010) Adaptation of *Fusarium graminearum* to tebuconazole yielded descendants diverging for levels of fitness, fungicide resistance, virulence, and mycotoxin production. *Phytopathology* **100:** 444–453.

Becher, R., Weihmann, F., Deising, H.B., and Wirsel, S.G. (2011) Development of a novel multiplex DNA microarray for *Fusarium graminearum* and analysis of azole fungicide responses. *BMC Genomics* **12:** 52.

Bond, L.M., Tumbarello, D.A., Kendrick-Jones, J., and Buss, F. (2013) Small-molecule inhibitors of myosin proteins. *Future Med Chem* **5:** 41–52.

Bruno, K.S., Tenjo, F., Li, L., Hamer, J.E., and Xu, J.R. (2004) Cellular localization and role of kinase activity of PMK1 in *Magnaporthe grisea*. *Eukaryot Cell* **3:** 1525–1532.

Chen, Y., and Zhou, M.G. (2009) Characterization of *Fusarium graminearum* isolates resistant to both carbendazim and a new fungicide JS399-19. *Phytopathology* **99:** 441–446.

Chen, Y., Chen, C., Zhou, M., Wang, J., and Zhang, W. (2009) Monogenic resistance to a new fungicide, JS399-19, in *Gibberella zeae*. *Plant Pathol* **58:** 565–570.

Chinthalapudi, K., Taft, M.H., Martin, R., Heissler, S.M., Preller, M., Hartmann, F.K., *et al*. (2011) Mechanism and specificity of pentachloropseudilin-mediated inhibition of myosin motor activity. *J Biol Chem* **286:** 29700–29708.

Crawley, S.W., Marc, A., Lee, S.-F., Li, Z., Chitayat, S., Smith, S.P., and Côté, G.P. (2006) Identification and characterization of an 8 kDa light chain associated with *Dictyostelium discoideum* MyoB, a class I myosin. *J Biol Chem* **281:** 6307–6315.

Dean, R., Van Kan, J.A., Pretorius, Z.A., Hammond-Kosack, K.E., Di Pietro, A., Spanu, P.D., *et al*. (2012) The Top 10 fungal pathogens in molecular plant pathology. *Mol Plant Pathol* **13:** 414–430.

Durrbach, A., Collins, K., Matsudaira, P., Louvard, D., and Coudrier, E. (1996) Brush border myosin I truncated in the motor domain impairs the distribution and the function of endocytic compartments in an hepatoma cell line. *Proc Natl Acad Sci USA* **93:** 7053–7058.

Geli, M.I., and Riezman, H. (1996) Role of type I myosins in receptor-mediated endocytosis in yeast. *Science* **272:** 533–535.

Goodson, H.V., Anderson, B.L., Warrick, H.M., Pon, L.A., and Spudich, J.A. (1996) Synthetic lethality screen identifies a novel yeast myosin I gene (MYO5): myosin I proteins are required for polarization of the actin cytoskeleton. *J Cell Biol* **133:** 1277–1291.

Jiang, J.H., Liu, X., Yin, Y.N., and Ma, Z.H. (2011) Involvement of a velvet protein FgVeA in the regulation of asexual development, lipid and secondary metabolisms and virulence in *Fusarium graminearum*. *PLoS ONE* **6:** e28291.

Jongeneel, C.V., Iseli, C., Stevenson, B.J., Riggins, G.J., Lal, A., Mackay, A., *et al*. (2003) Comprehensive sampling of gene expression in human cell lines with massively parallel signature sequencing. *Proc Natl Acad Sci USA* **100:** 4702–4705.

Kornt, E., and Pollard, T. (1993) Inhibition of contractile vacuole function in vivo by antibodies against myosin I. *Nature* **365:** 841–843.

Laakso, J.M., Lewis, J.H., Shuman, H., and Ostap, E.M. (2008) Myosin I can act as a molecular force sensor. *Science* **321:** 133–136.

Lee, W.L., Bezanilla, M., and Pollard, T.D. (2000) Fission yeast myosin I, Myo1p, stimulates actin assembly by Arp2/3 complex and shares functions with WASp. *J Cell Biol* **151:** 789–800.

Li, H., Diao, Y., Wang, J., Chen, C., Ni, J., and Zhou, M. (2008) JS399-19, a new fungicide against wheat scab. *Crop Prot* **27:** 90–95.

Li, X.D., Mabuchi, K., Ikebe, R., and Ikebe, M. (2004) Ca^{2+}-induced activation of ATPase activity of myosin Va is accompanied with a large conformational change. *Biochem Biophys Res Commun* **315:** 538–545.

Liu, X., Osherov, N., Yamashita, R., Brzeska, H., Korn, E.D., and May, G.S. (2001) Myosin I mutants with only 1% of wild-type actin-activated MgATPase activity retain essential in vivo function(s). *Proc Natl Acad Sci USA* **98:** 9122–9127.

Liu, X., Yin, Y.N., Wu, J.B., Jiang, J.H., and Ma, Z.H. (2010) Identification and characterization of carbendazim-resistant isolates of *Gibberella zeae*. *Plant Dis* **94:** 1137–1142.

Liu, X., Yu, F., Schnabel, G., Wu, J., Wang, Z., and Ma, Z. (2011) Paralogous *cyp51* genes in *Fusarium graminearum* mediate differential sensitivity to sterol demethylation inhibitors. *Fungal Genet Biol* **48:** 113–123.

Lu, Z.K., Shen, M., Cao, Y., Zhang, H.M., Yao, L.L., and Li, X.D. (2012) Calmodulin bound to the first IQ motif is responsible for calcium-dependent regulation of myosin 5a. *J Biol Chem* **287:** 16530–16540.

Ma, Z., and Michailides, T.J. (2005) Advances in understanding molecular mechanisms of fungicide resistance and molecular detection of resistant genotypes in phytopathogenic fungi. *Crop Prot* **24:** 853–863.

McGoldrick, C.A., Gruver, C., and May, G.S. (1995) myoA of *Aspergillus nidulans* encodes an essential myosin I

required for secretion and polarized growth. *J Cell Biol* **128:** 577–587.
McMullen, M., Bergstrom, G., De Wolf, E., Dill-Macky, R., Hershman, D., Shaner, G., and Van Sanford, D. (2012) A unified effort to fight an enemy of wheat and barley: *Fusarium* head blight. *Plant Dis* **96:** 1712–1728.
Mermall, V., Post, P.L., and Mooseker, M.S. (1998) Unconventional myosins in cell movement, membrane traffic, and signal transduction. *Science* **279:** 527–533.
Müllenborn, C., Steiner, U., Ludwig, M., and Oerke, E.C. (2008) Effect of fungicides on the complex of *Fusarium* species and saprophytic fungi colonizing wheat kernels. *Eur J Plant Pathol* **120:** 157–166.
Neuhaus, E.M., and Soldati, T. (2000) A myosin I is involved in membrane recycling from early endosomes. *J Cell Biol* **150:** 1013–1026.
Oberholzer, U., Marcil, A., Leberer, E., Thomas, D.Y., and Whiteway, M. (2002) Myosin I is required for hypha formation in *Candida albicans*. *Eukaryot Cell* **1:** 213–228.
Osherov, N., and May, G.S. (2000) In vivo function of class I myosins. *Cell Motil Cytoskeleton* **47:** 163–173.
Palchaudhuri, R., and Hergenrother, P.J. (2011) Transcript profiling and RNA interference as tools to identify small molecule mechanisms and therapeutic potential. *ACS Chem Biol* **6:** 21–33.
Pestka, J.J., and Smolinski, A.T. (2005) Deoxynivalenol: toxicology and potential effects on humans. *J Toxicol Environ Health B Crit Rev* **8:** 39–69.
Proctor, R.H., Hohn, T.M., and McCormick, S.P. (1995) Reduced virulence of *Gibberella zeae* caused by disruption of a trichothecene toxin biosynthetic gene. *Mol Plant Microbe Interact* **8:** 593–601.
Ramirez, M.L., Chulze, S., and Magan, N. (2004) Impact of environmental factors and fungicides on growth and deoxynivalenol production by *Fusarium graminearum* isolates from Argentinian wheat. *Crop Prot* **23:** 117–125.
Raposo, G., Cordonnier, M.N., Tenza, D., Menichi, B., Dürrbach, A., Louvard, D., and Coudrier, E. (1999) Association of myosin I alpha with endosomes and lysosomes in mammalian cells. *Mol Biol Cell* **10:** 1477–1494.
Sato, S.I., Murata, A., Shirakawa, T., and Uesugi, M. (2010) Biochemical target isolation for novices: affinity-based strategies. *Chem Biol* **17:** 616–623.
Son, H., Seo, Y.S., Min, K., Park, A.R., Lee, J., Jin, J.M., *et al*. (2011) A phenome-based functional analysis of transcription factors in the cereal head blight fungus, *Fusarium graminearum*. *PLoS Pathog* **7:** e1002310.
Steiner, B., Kurz, H., Lemmens, M., and Buerstmayr, H. (2009) Differential gene expression of related wheat lines with contrasting levels of head blight resistance after *Fusarium graminearum* inoculation. *Theor Appl Genet* **118:** 753–764.
Temesvari, L.A., Bush, J.M., Peterson, M.D., Novak, K.D., Titus, M.A., and Cardelli, J.A. (1996) Examination of the endosomal and lysosomal pathways in *Dictyostelium discoideum* myosin I mutants. *J Cell Sci* **109:** 663–673.
Wang, C., Zhang, S., Hou, R., Zhao, Z., Zheng, Q., Xu, Q., *et al*. (2011) Functional analysis of the kinome of the wheat scab fungus *Fusarium graminearum*. *PLoS Pathog* **7:** e1002460.
Wang, L.G., Ni, J.P., Wang, F.Y., Diao, Y.M., and Wei, P. (2004) The research on biological activities of new fungicide JS399-19. *Chin J Pestic* **43:** 380–383.
Xu, X., and Nicholson, P. (2009) Community ecology of fungal pathogens causing wheat head blight. *Annu Rev Phytopathol* **47:** 83–103.
Yamashita, R.A., and May, G.S. (1998) Constitutive activation of endocytosis by mutation of myoA, the myosin I gene of *Aspergillus nidulans*. *J Biol Chem* **273:** 14644–14648.
Yin, Y., Liu, X., Li, B., and Ma, Z. (2009) Characterization of sterol demethylation inhibitor-resistant isolates of *Fusarium asiaticum* and *F. graminearum* collected from wheat in China. *Phytopathology* **99:** 487–497.
Yu, J.H., Hamari, Z., Han, K.H., Seo, J.A., Reyes-Dominguez, Y., and Scazzocchio, C. (2004) Double-joint PCR: a PCR-based molecular tool for gene manipulations in filamentous fungi. *Fungal Genet Biol* **41:** 973–981.
Zhang, Y.J., Zhang, X., Chen, C.J., Zhou, M.G., and Wang, H.C. (2010) Effects of fungicides JS399-19, azoxystrobin, tebuconazloe, and carbendazim on the physiological and biochemical indices and grain yield of winter wheat. *Pestic Biochem Phys* **98:** 151–157.

Supporting information

Additional Supporting information may be found in the online version of this article at the publisher's web-site:

Fig. S1. Inhibitory effect of carbendazim, tebuconazole and JS399-19 against *F. graminearum* and *F. asiaticum*.
A. Chemical structure of the novel fungicide JS399-19.
B. *Fusarium graminearum* strain PH-1 and *F. asiaticum* strain GJ33 were inoculated onto the PDA plates supplemented with 0.3 μg ml^{-1} tested fungicides. The solvent DMSO was used as a control. Inoculated plates were photographed after 3 days incubation at 25°C.
Fig. S2. Inhibitory effect of JS399-19 against conidial germination of *F. graminearum* and *Magnaporthe grisea* after 2, 4 or 8 h of incubation.
Fig. S3. The transcription level of the beta-tubulin gene (*TUB2*) in *F. graminearum* PH-1 treated with carbendazim. The relative transcription level of *TUB2* in PH-1 treated with 10 μg ml^{-1} carbendazim is the relative amount of mRNA of the gene in PH-1 without carbendazim treatment (CK).
Fig. S4. JS399-19-resistant (JS-R) mutants obtained by UV irradiation contain the point mutations at codon 217 and 420 of FgMyo1.
A. The mutants (JS-R-1 to 10) and the wild-type PH-1 were incubated on PDA amended with 1 or 100 μg ml^{-1} JS399-19. The solvent DMSO was used as a control.
B. Alignment of partial deduced amino acid sequences of FgMyo1 from the wild-type PH-1 and JS-R mutants. The vertical boxes indicate the amino acid changes at the codons 217 and 420 that are responsible for JS399-19 resistance.
C. Predicted domains of FgMyo1 protein. Line represents the full-length 1129-amino-acid protein. The boxes represent the identified domains and were labelled with different colors.
D. Locations of point mutations S217L and E420K in the putative FgMyo1 structure, which was constructed based on the crystal structure of *Dictyostelium discoideum* myosin IE

motor domain (PDB code 1LKX). Green, 25 kDa domain; red, upper 50 kDa domain; white, lower 50 kDa domain, blue, 20 kDa domain; spheres, Mg^{2+}.ADP.VO_4. Structure model of FgMyo1 was constructed using the PyMOL Molecular Graphics System software (DeLano Scientific, San Carlos, CA, USA).

Fig. S5. Southern blotting assays of FgMyo1 in the wild-type PH-1 and the strains derived from PH-1.

Fig. S6. Alignments of amino acid sequences of Myo1 from different fungi, including *Fusarium graminearum* (FgMyo1), *Fusarium verticillioides* (FvMyo1), *Fusarium oxysporum* (FoMyo1), *Fusarium solani* (FsMyo1), *Magnaporthe grisea* (MgMyo1), *Botrytis cinerea* (BcMyo1), *Aspergillus flavus* (AfMyo1) and *Saccharomyces cerevisiae* (ScMyo1). The vertical blue and red boxes indicate the amino acid residues corresponding to the S217 and E420 of FgMyo1 respectively.

Fig. S7. SDS-PAGE (4–20%) of the purified FgMyo1-MIQ^{WT}, FgMyo1-MIQ^{S217L} and FgMyo1-MIQ^{E420K}. The arrowhead indicates the target protein.

Table S1. A list of 156 genes upregulated by JS399-19 treatment in the wild-type PH-1.

Table S2. PCR primers used in this study.